PHYSICAL REVIEW A VOLUME 26, NUMBER 5 NOVEMBER 1982

Nonlinear theory of the free-electron laser with an axial magnetic field

Lazar Friedland and Ira B. Bernstein
Department of Applied Physics, Yale University, New Haven, Connecticut 06520
(Received 17 December 1981)

A nonlinear, one-dimensional formulation of the free-electron laser with an axial magnetic field is presented. The problem is formulated in the cold-fluid approximation for the electron beam, and is reduced to a system of the first-order, nonlinear, coupled, ordinary differential equations. Nonlinear effects due to the departure of the electrons in the beam from the conventional helical orbits are considered and illustrated in numerical examples. The formalism also allows the study of the initial phase of saturation in the laser. In the presence of the axial magnetic field the saturation is shown to be mainly due to the development of undesirable large radial excursion of the electron trajectories.

I. INTRODUCTION

Free-electron lasers operating in the Raman regime are believed to be promising sources of intense submillimeter coherent radiation. This prediction was tested in experiments at the Navy Research Laboratory (NRL) and Columbia University,[1-4] and recently with improved electron beam quality at NRL.[5,6] The Raman free-electron lasers operate with relatively low electron energies (relativistic $\gamma < 10$) and high beam currents ($I > 1$ kA). These experimental conditions, especially the high beam currents, necessarily require the presence of an axial guide magnetic field, in addition to the magnetic wiggler, conventionally used in free-electron laser experiments. As was demonstrated in recent theoretical studies by Friedland *et al.*,[7-10] the simple addition of the guide field results in many nontrivial consequences. For example, in the presence of the guide field electron trajectories may become very complex, and, only for certain combinations of injection conditions on the electron beam, the electrons will move on simple helical orbits.[7] Moreover, even on the helical orbits, in combined guide and wiggler magnetic fields, the beam response to perturbations is characterized by an additional response frequency, which may be varied without changing the helical orbit itself. It was shown in the single-particle theory of the laser[8] that the resonance between this natural response frequency and the frequency of a driving electromagnetic wave can be exploited to provide higher gain in the system. These predictions were confirmed by the self-consistent collective theories[9,10] which also demonstrated the presence of additional effects. For example, under certain conditions, the frequency range of the free-electron laser instability may be substantially extended to both lower and higher frequencies. The effect was explained in Ref. 10 by the presence of an unstable beam mode in the system.

All this complex behavior, induced by the presence of the guide field in the system, has been studied in Refs. 7-10 on the basis of linearized theories. The linearization procedure itself was based on two assumptions. First of all it was assumed that the perturbing electromagnetic fields were so weak that all the induced nonlinear effects were small and could be neglected. Second, the assumption was made that the unperturbed electron beam propagated on one of the helical orbits [branches A or C (Refs. 8-10)] and the linearized perturbation analysis was performed around these steady-state trajectories. Both these assumptions impose serious limitations on the theory. Indeed, the linear theories predicted the possibility of very high gains, so that the nonlinear electromagnetic effect might become important and lead to saturation after the radiation traversed a relatively short distance. Moreover, as was already mentioned, the helical orbits, in the presence of the guide magnetic field, are exceptions rather than the rule. In case of a departure of the beam from the helical orbits, the electron dynamics becomes intrinsically nonlinear, which may play an important role in realistic systems even when the radiation fields are weak.

In this paper we present a nonlinear theory of the free-electron laser with the guide field and consider both aforementioned nonlinear effects. A nonlinear theory for the laser without the guide field was

given by Sprangle *et al.*[11,12] Their approach was primarily designed to study saturation effects due to particle trapping in the ponderomotive potential of the wave and the wiggler field. The trapping occurs on a scale length comparable to the wavelength of the electromagnetic wave. The number of test particles, separated initially by distances short compared to the period of the wave, were necessary to model the saturation effects. Here we present a more simple approach based on the cold-fluid model of the electron beam. The method requires one to follow only one test particle along the laser. Although the trapping effect, in principle, cannot be described by our formalism, its use is very convenient in describing all the effects occurring on the scale length long compared to the wavelength. We will show that in the presence of the guide field, both the departure from the helical orbits and the initial saturation phase belong to this class of slowly varying effects, and thus can be treated within the cold-fluid approximation.

The scope of the paper is as follows. In Sec. II we derive a reduced system of equations for the amplitude of the radiation field. In Sec. III we consider the momentum equation defining the sources in the field equations. A complete set of first-order, coupled, nonlinear ordinary differential equations governing our system will be presented at the end of Sec. III. This set of equations, in Sec. IV, will form a basis for the discussion of possible nonlinear effects in the system, which will be illustrated by numerical examples.

II. FIELD EQUATIONS

Consider a one-dimensional model of a free-electron laser, where the electromagnetic field is described by the Maxwell equations

$$c\vec{e}_z\times\frac{\partial\vec{B}_\perp}{\partial z}=\frac{\partial\vec{E}_\perp}{\partial t}-4\pi e(N\vec{V}_\perp-\langle N\vec{V}_\perp\rangle_{\rm av}) , \tag{1}$$

$$-c\vec{e}_z\times\frac{\partial\vec{E}_\perp}{\partial z}=\frac{\partial\vec{B}_\perp}{\partial t} , \tag{2}$$

$$\frac{\partial E_z}{\partial t}=4\pi e(NV_z-\langle NV_z\rangle_{\rm av}) , \tag{3}$$

$$\frac{\partial B_z}{\partial t}=0 , \tag{4}$$

$$\frac{\partial E_z}{\partial z}=-4\pi e(N-\langle N\rangle_{\rm av}) , \tag{5}$$

$$\frac{\partial B_z}{\partial z}=0 . \tag{6}$$

Here the electron beam propagates in the z direction and is described in the cold-fluid approximation. The electron beam density N and velocity $\vec{V}$, and the electromagnetic fields $\vec{E}$ and $\vec{B}$, in Eqs. (1)–(6) are assumed to depend only on z and time, and the subscript $\perp$ describes directions perpendicular to the z axis. Moreover, we are interested in solutions of (1)–(6) periodic in time with period $2\pi/\omega$ and consequently subtract off the time-averaged parts

$$\langle N\vec{V}\rangle_{\rm av}=\frac{\omega}{2\pi}\int_0^{2\pi/\omega}N\vec{V}\,dt ,$$
$$\langle N\rangle_{\rm av}=\frac{\omega}{2\pi}\int_0^{2\pi/\omega}N\,dt , \tag{7}$$

of the sources in Eqs. (1), (3), and (5).

The periodicity condition allows one to expand the electromagnetic fields in the Fourier series

$$\vec{E}(z,t)=\tfrac{1}{2}\sum_{\substack{n=-\infty\\ n\neq 0}}^{+\infty}\vec{E}_n(z)e^{-in\omega t}$$
$$=\sum_{n=1}^{\infty}{\rm Re}[\vec{E}_n(z)e^{-in\omega t}] ,$$
$$\vec{B}(z,t)=\sum_{n=1}^{\infty}{\rm Re}[\vec{B}_n(z)e^{-in\omega t}] . \tag{8}$$

We assume now that only the $n=1$ component in (8) is excited, which is the usual case in free-electron lasers operating in the linear regime. The coupling to higher harmonics is a second-order nonlinear effect, as can be seen from Eqs. (1) and (3), and we will neglect this effect in the present work. Thus we write

$$\vec{E}(z,t)={\rm Re}[\vec{E}_1(z)e^{-i\omega t}] ,$$
$$\vec{B}(z,t)={\rm Re}[\vec{B}_1(z)e^{-i\omega t}] , \tag{9}$$

and accordingly

$$N(z,t)=N_0(z)+{\rm Re}[N_1(z)e^{-i\omega t}] ,$$
$$\vec{V}(z,t)=\vec{V}_0(z)+{\rm Re}[\vec{V}_1(z)e^{-i\omega t}] . \tag{10}$$

We also assume here that ω is much larger than various characteristic frequencies of the electron beam (such as the plasma frequency ω_p, the undulation frequency, the natural response frequency,[8] etc.). Then we can separate "fast" spatial oscillations in (9) and (10) from the slow ones which are imposed by the presence of the electron beam. Namely, we write

$$\vec{E}_1(z)=\frac{mc^2}{e}\vec{a}(z)e^{i(\omega/c)z},$$
$$\vec{B}_1(z)=\frac{mc^2}{e}\vec{b}(z)e^{i(\omega/c)z},$$
$$N_1(z)=\frac{m}{4\pi e^2}\nu^2(z)e^{i(\omega/c)z}, \tag{11}$$
$$\vec{V}_1(z)=\vec{v}(z)e^{i(\omega/c)z},$$

where in order of magnitude for $X=a,b,\nu^2,v$,

$$\left|\frac{d\ln X}{dz}\right|\ll\frac{\omega}{c}. \tag{12}$$

Note that at this point we have excluded from the analysis all waves with wave vectors in the direction opposite to the direction of propagation of the electron beam. These backward waves can only arise from noise and their amplitudes are assumed to be negligible in comparison with the main amplified signal which propagates in the direction of the beam. Although in some cases the backward waves are absolutely unstable[13] they are characterized in such cases by long wavelengths and therefore can be easily suppressed by appropriate construction of the amplifier cavity.[13]

We now proceed to the derivation of the approximate equations, describing the slowly varying amplitudes of the electromagnetic fields. First, we combine (1) and (2) to give the wave equation

$$\frac{\partial^2\vec{E}_\perp}{\partial z^2}-\frac{1}{c^2}\frac{\partial^2\vec{E}_\perp}{\partial t^2}=-\frac{4\pi e}{c^2}\frac{\partial}{\partial t}(N\vec{V}_\perp). \tag{13}$$

Substituting (9) and (10) into (13), applying definitions (11), and neglecting the higher-frequency harmonics, we get

$$\frac{d^2\vec{a}_\perp}{dz^2}+2i\frac{\omega}{c}\frac{d\vec{a}_\perp}{dz}=i\frac{\omega}{c^4}(\omega_p^2\vec{v}_\perp+\vec{V}_{0\perp}\nu^2). \tag{14}$$

Finally, exploiting the assumption of the weakness of the z dependence of $d\vec{a}_\perp/dz$, we neglect the second-order derivative in Eq. (14) and rewrite it in the approximate form

$$\frac{d\vec{a}_\perp}{dz}=\frac{1}{2c^3}(\omega_p^2\vec{v}_\perp+\vec{V}_{0\perp}\nu^2). \tag{15}$$

In the notation of (11), Eq. (5) becomes

$$\frac{da_z}{dz}+i\frac{\omega}{c}a_z=-\frac{\nu^2}{c^2} \tag{16}$$

and (3) can be written as

$$-i\frac{\omega}{c}a_z-\frac{1}{c^3}(\omega_p^2 v_z+V_{0z}\nu^2)=0. \tag{17}$$

On expressing ν^2 via (17), and substituting it into (16) we have

$$\left[-i\frac{\omega}{c}\left[1-\frac{V_{0z}}{c}\right]+\frac{V_{0z}}{c}\frac{d}{dz}\right]a_z=\frac{\omega_p^2}{c^2}\frac{v_z}{c}. \tag{18}$$

Note that in (18)

$$\frac{\omega}{c}\left[1-\frac{V_{0z}}{c}\right]\simeq\frac{\omega}{c}\frac{1}{2\gamma_z^2},$$

where γ_z is the relativistic factor associated with the axial velocity of the electron beam. Therefore for $\omega/c\simeq 2\gamma_z^2 k_0$, which is characteristic of free-electron lasers with a pitch $\lambda=2\pi/k_0$, we have

$$\frac{\omega}{c}\left[1-\frac{V_{0z}}{c}\right]\simeq k_0$$

and thus (18) indeed describes variation of $a_z(z)$ on a scale long compared with the fast oscillations of the electromagnetic field.

Equation (17) can be also used to eliminate ν^2 from Eq. (15), which then becomes

$$\frac{d\vec{a}_\perp}{dz}=\frac{1}{2c^3}\left[\omega_p^2\vec{v}_\perp-\frac{\vec{V}_{0\perp}}{V_{0z}}(\omega_p^2 v_z+i\omega c^2 a_z)\right]. \tag{19}$$

The form of the operator in the square brackets in Eq. (18) suggests the use of an independent variable other than z, namely, we introduce variable τ via

$$\frac{dz}{d\tau}=V_{0z}(z). \tag{20}$$

Then for any quantity of the form

$$\tilde{X}(z,\tau)=X(z)e^{i(\omega/c)(z-c\tau)} \tag{21}$$

we have

$$\frac{1}{c}\frac{d\tilde{X}}{d\tau}=\frac{1}{c}\left[\frac{\partial}{\partial\tau}+V_{0z}\frac{\partial}{\partial z}\right]\tilde{X}$$
$$=e^{i(\omega/c)(z-c\tau)}\left[-i\frac{\omega}{c}\left[1-\frac{V_{0z}}{c}\right]+\frac{V_{0z}}{c}\frac{d}{dz}\right]X. \tag{22}$$

Therefore (18) can be rewritten as

$$\frac{1}{c}\frac{d\tilde{a}_z}{d\tau}=\frac{\omega_p^2}{c^3}\tilde{v}_z. \tag{23}$$

In addition to simplifying the notation, τ has an im-

portant physical interpretation: It measures the time along the trajectory were the electron to move with velocity $V_{0z}(z)$. As we will show in the next section, convective derivatives similar to $d/d\tau$ in Eq. (23) appear naturally in the momentum equation for the electron beam. Thus, in the following we will adopt τ as the independent variable in the problem. Consistent with this approach we also rewrite Eq. (19) in the form

$$\frac{1}{c}\frac{d\tilde{\vec{a}}_\perp}{d\tau}=-i\frac{\omega}{c}\left[1-\frac{V_{0z}}{c}\right]\tilde{\vec{a}}_\perp + \frac{1}{2c^4}[\omega_p^2 V_{0z}\tilde{\vec{v}}_\perp-\vec{V}_{0\perp}(\omega_p^2\tilde{v}_z+i\omega c^2\tilde{a}_z)] \ . \tag{24}$$

Equations (23) and (24) are the desired equations for the electromagnetic field.

III. MOMENTUM EQUATION

Consider the momentum equation describing the electron beam

$$\left[\frac{\partial}{\partial t}+V_z\frac{\partial}{\partial z}\right](\gamma\vec{V})=-\frac{e}{m}\left[\vec{E}+\frac{\vec{V}}{c}\times(\vec{B}+\vec{\mathscr{B}})\right], \tag{25}$$

where the static magnetic field is given by

$$\vec{\mathscr{B}}(z)=-\hat{e}_\perp(z)\mathscr{B}_\perp+\hat{e}_z\mathscr{B}_z \tag{26}$$

with the vector

$$\hat{e}_\perp(z)=-(\hat{e}_x\cos k_0 z+\hat{e}_y\sin k_0 z) \tag{27}$$

representing the direction of the helical field on the axis of a magnetic wiggler commonly used in theories of free-electron lasers. Substituting (9) and (10) into (25), using definitions (11), and retaining only the first-time harmonic in the resulting equation, we have

$$\gamma_0\dot{\vec{v}}+\vec{V}_0\dot{g}+v_z\frac{d}{dz}(\gamma_0\vec{V}_0)+V_{0z}\left[g\frac{d\vec{V}_0}{dz}+\vec{v}\frac{d\gamma_0}{dz}\right]+\frac{i}{2}\frac{\omega}{c}v_z^*\vec{v}g=-c^2\left[\vec{a}+\frac{\vec{V}_0}{c}\times\vec{b}\right]-\vec{v}\times\vec{\Omega} \ . \tag{28}$$

Here we defined $\Omega=e\vec{\mathscr{B}}/mc$,

$$\gamma=\gamma_0+\mathrm{Re}[g(z)e^{i(\omega/c)(z-ct)}] \tag{29}$$

and $(\cdots)^{\cdot}=[-i\omega(1-V_{0z}/c)+V_{0z}d/dz](\cdots)$. In the last term on the left-hand side of Eq. (28), which is the only nonlinear term of the third order, in view of (12), we have neglected $d\vec{v}/dz$ and dg/dz compared with $i(\omega/c)\vec{v}$ and $i(\omega/c)g$, respectively. An equation for the quantity $\dot{g}$ in (28) is obtained from the energy balance

$$mc^2\left[\frac{\partial}{\partial t}+V_z\frac{\partial}{\partial z}\right]\gamma=-e\vec{V}\cdot\vec{E} \tag{30}$$

which yields

$$\dot{g}=-v_z\frac{d\gamma_0}{dz}-\vec{V}_0\cdot\vec{a} \ . \tag{31}$$

Also, it follows from (2), that

$$\vec{b}_\perp=-i\frac{c}{\omega}\hat{e}_z\times\left[i\frac{\omega}{c}\vec{a}_\perp+\frac{d\vec{a}_\perp}{dz}\right] . \tag{32}$$

Then in (28)

$$\left[\vec{a}+\frac{\vec{V}_0}{c}\times\vec{b}\right]=\frac{ic}{\omega}\dot{\vec{a}}_\perp+\hat{e}_z\left[\frac{\vec{V}_{0\perp}}{c}\cdot\left[\vec{a}_\perp-i\frac{c}{\omega}\frac{d\vec{a}_\perp}{dz}\right]+a_z\right]\simeq\frac{ic}{\omega}\dot{\vec{a}}_\perp+\hat{e}_z\left[\frac{\vec{V}_{0\perp}}{c}\cdot\vec{a}_\perp+a_z\right] . \tag{33}$$

The appearance of the dotted quantities in Eqs. (28), (31), and (33) suggests that one change from the variable z in these equations to the time τ along the steady (time-independent) component of the electron motion in the z direction [see the definition in Eq. (20)]. Then, on using notation (21), observing that $\dot{X}\exp[i(\omega/c)(z-ct)]=d\tilde{X}/d\tau$ and $V_{0z}dX/dz=dX/d\tau$, and substituting (33) into (28) we get

$$\gamma_0\frac{d\vec{v}'}{d\tau}=-\vec{V}_0\frac{dg}{d\tau}-\vec{v}'\times\vec{\Omega}-\frac{ic^3}{\omega}\frac{d\tilde{\vec{a}}_\perp}{d\tau}-c^2\hat{e}_z\left[\frac{\vec{V}_{01}}{c}\cdot\tilde{\vec{a}}+\tilde{a}_z\right]$$

$$-\frac{\tilde{v}_z}{V_{0z}}\frac{d}{d\tau}(\gamma_0\vec{V}_0)-\tilde{g}\frac{d\vec{V}_0}{d\tau}-\vec{v}'\frac{d\gamma_0}{d\tau}+\frac{i\omega}{2c}\tilde{v}_z^*\vec{v}'\tilde{g}\ , \tag{34}$$

where $\vec{v}'$ has components $\tilde{v}_x$, $\tilde{v}_y$, and $\tilde{v}_z$, etc., and where according to (31)

$$\frac{d\tilde{g}}{d\tau}=-\frac{\tilde{v}_z}{V_{0z}}\frac{d\gamma_0}{d\tau}-\vec{V}_0\cdot\tilde{\vec{a}}\ . \tag{35}$$

Because of the form of the helical part of the magnetostatic field $\vec{\mathscr{B}}$ it is convenient in the following to introduce a rotating coordinate system defined by the base vectors

$$\hat{e}_1=-\hat{e}_x\sin k_0z+\hat{e}_y\cos k_0z,\quad \hat{e}_2=\hat{e}_\perp\ ,$$
$$\hat{e}_3=\hat{e}_z\ . \tag{36}$$

Then, finally, components in Eqs. (23), (24), (34), and (35) become

$$\frac{d\tilde{a}_1}{d\tau}=k_0V_{03}\tilde{a}_2-i\omega\left[1-\frac{V_{03}}{c}\right]\tilde{a}_1+\frac{1}{2c^3}[\omega_p^2V_{03}\tilde{\gamma}_1-V_{01}(\omega_p^2\tilde{v}_3+i\omega c^2\tilde{a}_3)]\ , \tag{37}$$

$$\frac{d\tilde{a}_2}{d\tau}=-k_0V_{03}\tilde{a}_1-i\omega\left[1-\frac{V_{03}}{c}\right]\tilde{a}_2+\frac{1}{2c^3}[\omega_p^2V_{02}\tilde{v}_2-V_{02}(\omega_p^2\tilde{v}_3+i\omega c^2\tilde{a}_3)]\ , \tag{38}$$

$$\frac{d\tilde{a}_3}{d\tau}=\frac{\omega_p^2}{c^2}\tilde{v}_3\ , \tag{39}$$

$$\gamma_0\frac{d\tilde{v}_1}{d\tau}=\gamma_0k_0V_{03}\tilde{v}_2-V_{01}\frac{d\tilde{g}}{d\tau}-\Omega_\perp\tilde{v}_3-\Omega_{||}\tilde{v}_2-\frac{ic^3}{\omega}\left[\frac{d\tilde{a}_1}{d\tau}-k_0V_{03}\tilde{a}_2\right]-\frac{\tilde{v}_3}{V_{03}}\left[\frac{d}{d\tau}(\gamma_0V_{01})-\gamma_0k_0V_{02}V_{03}\right]$$

$$-\tilde{g}\left[\frac{dV_{01}}{d\tau}-k_0V_{02}V_{03}\right]-\tilde{v}_1\frac{d\gamma_0}{d\tau}+\frac{i\omega}{2c}\tilde{v}_3^*\tilde{v}_1\tilde{g}\ , \tag{40}$$

$$\gamma_0\frac{d\tilde{v}_2}{d\tau}=-\gamma_0k_0V_{03}\tilde{v}_1-V_{02}\frac{d\tilde{g}}{d\tau}+\Omega_{||}\tilde{v}_1-\frac{ic^3}{\omega}\left[\frac{d\tilde{a}_2}{d\tau}+k_0V_{03}\tilde{a}_1\right]-\frac{\tilde{v}_3}{V_{03}}\left[\frac{d}{d\tau}(\gamma_0V_{02})+\gamma_0k_0V_{01}V_{03}\right]$$

$$-\tilde{g}\left[\frac{dV_{02}}{d\tau}+k_0V_{01}V_{03}\right]-\tilde{v}_2\frac{d\gamma_0}{d\tau}+\frac{i\omega}{2c}\tilde{v}_3^*\tilde{v}_2\tilde{g}\ , \tag{41}$$

$$\gamma_0\frac{d\tilde{v}_3}{d\tau}=(c-V_{03})\left[\frac{d\tilde{g}}{d\tau}-c\tilde{a}_3\right]+\frac{c\tilde{v}_3}{V_{03}}\frac{d}{d\tau}\left[\gamma_0\left[1-\frac{V_{03}}{c}\right]\right]+\Omega_\perp\tilde{v}_1-\tilde{v}_3\frac{d\gamma_0}{d\tau}-\tilde{g}\frac{dV_{03}}{d\tau}+\frac{i\omega}{2c}\tilde{v}_3^*\tilde{v}_3\tilde{g}\ , \tag{42}$$

$$\frac{d\tilde{g}}{d\tau}=V_{01}\tilde{a}_1-V_{02}\tilde{a}_2-V_{03}\tilde{a}_3-\frac{\tilde{v}_3}{V_{03}}\frac{d\gamma_0}{d\tau}\ . \tag{43}$$

Equations (32)–(43) describe the nonlinear evolution of the time-dependent parts of various quantities characterizing the free-electron laser. These equations are combined here into a system of first-order, nonlinear, coupled differential equations, which can be solved numerically with an appropriate set of initial conditions. In order to do so, we still have to complete this system by the equations for the steady (time-independent) parts of various quantities ($\omega_p,\gamma_0,\vec{V}_0$). One such equation is ob-

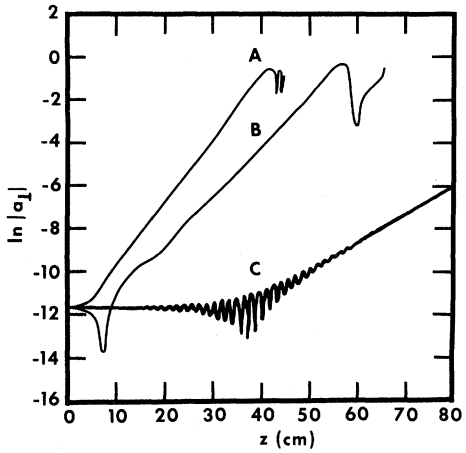

FIG. 1. Dependence of the absolute value of the perpendicular component of the electric field on z. A: $r=0.868$ (branch A) $\omega/c=75$ cm^{-1}. B: $r=1.077$ (branch C), $\omega/c=75$ cm^{-1}. C: $r=1.077$, $\omega/c=130$ cm^{-1}. In all the examples $\omega_p^2/c^2=0.5$ cm^{-2}, $\gamma_0=3$, $k_0=6$ cm^{-1}, and $\xi=0.5$.

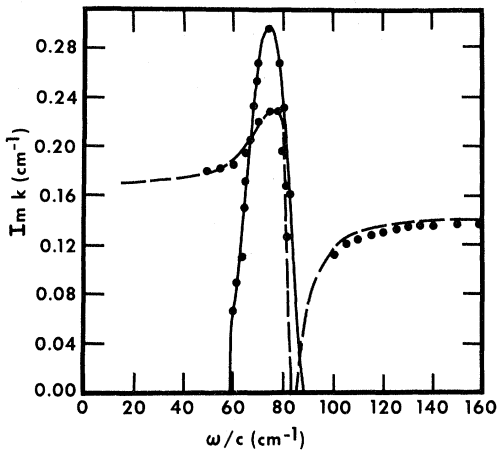

FIG. 2. Spatial growth rates (Imk) vs ω/c in the linear regimes in the sample case. Solid and dashed lines are the results of the linear theory (Ref. 9) for $r=0.868$ and $r=1.077$, respectively. The dots are the results of the present calculations.

tained from the continuity equation

$$\frac{\partial N}{\partial t}+\frac{\partial}{\partial z}(NV_z)=0\ , \tag{44}$$

the time-independent part of which is

$$\frac{d}{dz}(\omega_p^2 V_{0z}+\langle \nu^2 v_z\rangle_+)=0\ , \tag{45}$$

or, on using (17)

$$\omega_p^2 V_{03}=(\omega_p^2 V_{03})\,|_{\tau=0}+\frac{1}{V_{03}}(\omega_p^2\langle \tilde{v}_3\tilde{v}_3\rangle_+ +\omega c^2\langle \tilde{a}_3\tilde{v}_3\rangle_-)\ , \tag{46}$$

where we have used the notations

$$\langle\alpha\beta\rangle_+=\tfrac{1}{2}\,\mathrm{Re}(\alpha^*\beta)\ ,\qquad \langle\alpha\beta\rangle_-=\tfrac{1}{2}\,\mathrm{Im}(\alpha^*\beta)\ . \tag{47}$$

Similarly to (45) the steady part of (30) gives

$$\frac{d\gamma_0}{d\tau}\simeq\frac{\omega}{c}\langle \tilde{v}_3\tilde{g}\rangle_- -\langle \tilde{v}_1\tilde{a}_1\rangle_+ -\langle \tilde{v}_2\tilde{a}_2\rangle_+ -\langle \tilde{v}_2\tilde{a}_3\rangle_+\ . \tag{48}$$

And, finally, an equation for $\vec{V}_0$ is obtained by considering the steady part of the momentum equation (25), which can be written in components as

$$\frac{dV_{01}}{d\tau}=V_{02}\left[k_0V_{03}-\frac{\Omega_{||}}{\gamma_0}\right]-\frac{\Omega_\perp}{\gamma_0}V_{03}+\frac{\Delta_1}{\gamma_0}\ , \tag{49}$$

$$\frac{dV_{02}}{d\tau}=-V_{01}\left[k_0V_{03}-\frac{\Omega_{||}}{\gamma_0}\right]+\frac{\Delta_2}{\gamma_0}\ , \tag{50}$$

$$\frac{dV_{03}}{d\tau}=V_{01}\frac{\Omega_\perp}{\gamma_0}+\frac{\Delta_3}{\gamma_0}\ , \tag{51}$$

where

$$\Delta_1\simeq -V_{01}\frac{d\gamma_0}{d\tau}+\frac{\omega}{c}(\gamma_0\langle \tilde{v}_3\tilde{v}_1\rangle_- +V_{01}\langle \tilde{v}_3\tilde{g}\rangle_-)+k_0(V_{02}\langle \tilde{v}_3\tilde{g}\rangle_+ +V_{03}\langle \tilde{v}_2\tilde{g}\rangle_+ +\gamma_0\langle \tilde{v}_2\tilde{v}_3\rangle_+)+c\langle \tilde{v}_3\tilde{a}_1\rangle_+\ , \tag{52}$$

$$\Delta_2\simeq -V_{02}\frac{d\gamma_0}{d\tau}+\frac{\omega}{c}(\gamma_0\langle \tilde{v}_3\tilde{v}_2\rangle_- +V_{02}\langle \tilde{v}_3\tilde{g}\rangle_-)-k_0(V_{01}\langle \tilde{v}_3\tilde{g}\rangle_+ +V_{03}\langle \tilde{v}_1\tilde{g}\rangle_+ +\gamma_0\langle \tilde{v}_3\tilde{v}_1\rangle_+)+c\langle \tilde{v}_3\tilde{a}_2\rangle_+\ , \tag{53}$$

$$\Delta_3\simeq -V_{03}\frac{d\gamma_0}{d\tau}-\frac{\omega}{c}\langle \tilde{v}_3\tilde{g}\rangle_- -c(\langle \tilde{v}_1\tilde{a}_1\rangle_+ +\langle \tilde{v}_2\tilde{a}_2\rangle_+)\ . \tag{54}$$

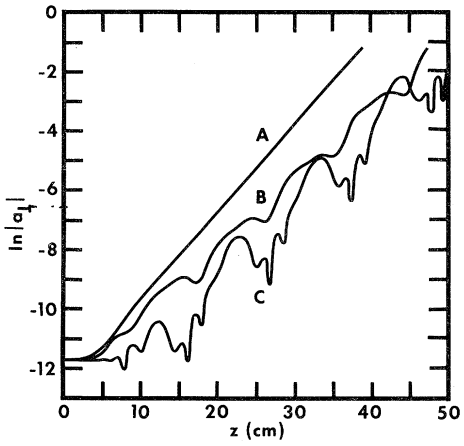

FIG. 3. Effects of the departure from the steady-state trajectories on the gain in the amplifier in the sample case. All the curves correspond to initial value of $r=0.868$ and $\omega/c=75$ cm^{-1}. *A*: $\psi=0$. *B*: $\psi=0.1$. *C*: $\psi=0.3$.

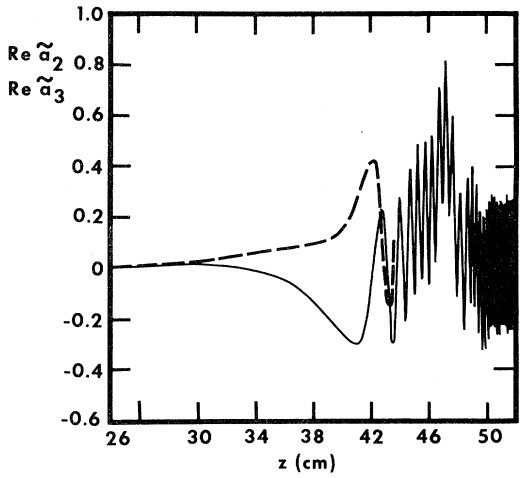

FIG. 5. z dependence of real parts of $\tilde{a}_2$ (the solid line) and $\tilde{a}_3$ (the dashed line) in the saturation phase. The parameters are $\omega/c=75$ cm^{-1}, $\psi=0$, $r=0.868$.

IV. NUMERICAL EXAMPLES

In the following numerical applications we will consider the case where $k_0=6$ cm^{-1} and initially the beam is characterized by $\gamma_0=3$ and $\omega_p^2/c^2=0.5$ cm^{-2}. This sample case has been studied in the recent linear theory of the laser,[9] and therefore provides a convenient example of our nonlinear formulation.

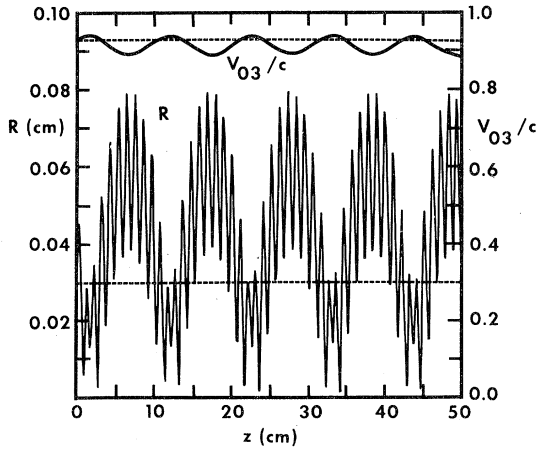

FIG. 4. Axial, time-independent component of the velocity V_{03} and electron displacement R vs z in the sample case. Initially (at $z=0$) in the figure $r=0.868$ and $\omega/c=75$ cm^{-1}. The dashed lines represent the case $\psi=0$ (steady-state trajectories) and the solid lines correspond to $\psi=0.3$.

As a first application we will assume that as in Ref. 9 the electron beam enters the interaction region on one of the two possible "steady-state" helical orbits (branches *A* and *C* of Ref. 9). These two regimes are characterized in the linear theory by different ranges of parameter $r=\Omega_{||}/\gamma_0 k_0 V_{03}$ (on branch *A*, $r<1$, while on branch *C*, $r>1$). In these calculations we will change r by varying $\Omega_{||}$. We will simultaneously adjust $\Omega_\perp$ so that in all the examples, initially at $\tau=0$, we will have $V_{0\perp}/c=\xi/\gamma_0$ with $\xi=0.5$. In Fig. 1 we present some typical results of the nonlinear calculations of the evolution of the absolute value of the perpendicular component of the electric field $|\tilde{a}_\perp|$ along the amplifier. The cases $r=0.868$ (branch *A*) with $\omega/c=75$ cm^{-1} and $r=1.077$ (branch *C*) with $\omega/c=75$ cm^{-1}, 130 cm^{-1} are shown. It can be seen in the figure that the evolution of the electromagnetic signal in the device passes through the qualitatively different stages. At short distances the interference of the linear modes in the system leads to a nontrivial occasionally oscillatory dependence of $|\tilde{a}_\perp|$ on z. At longer distances the electromagnetic gain in the amplifier is linear and the corresponding slopes of the curves in Fig. 1 are determined by the maximum spatial growth rate (Imk) in the system as described in the linear theory. Finally, when the intensity of the wave becomes large enough, the nonlinear effects start playing a major role and the wave enters the saturation stage. We will discuss the saturation effects in our system later in this section and now proceed with a more detailed comparison with the results of the linear theory. Figure 2

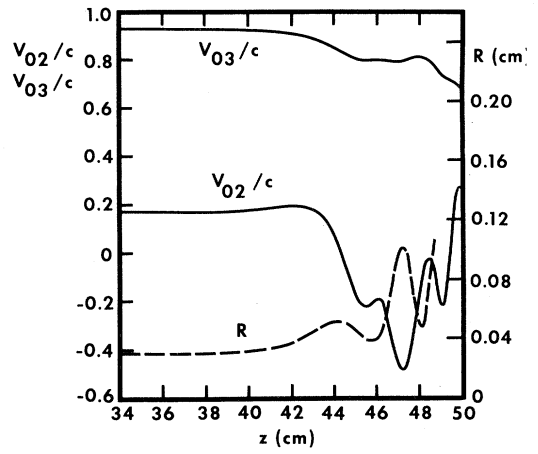

FIG. 6. Time-independent components V_{02}, V_{03}, and radial displacement R vs z in the saturation phase in the amplifier. The curves correspond to the case $\omega/c=75$ cm^{-1}, $\psi=0$, $r=0.868$.

presents such a comparison. The frequency dependence of the linear spatial growth rates on branches A ($r=0.868$) and C ($r=1.077$), shown in this figure has been obtained from the results similar to those shown in Fig. 1. An excellent agreement with the linear theory[9] is obvious.

Next we proceed to the study of nonlinear effects. First consider the effects due to the departure of the beam from the steady-state branches A and C. This situation is likely to occur in experiments as a result of an inaccurate alignment of the direction of injection of the beam into the amplifier. In Fig. 3 we demonstrate the effects on the gain of the departure from the helical orbits. We present the case of $\omega/c=75$ cm^{-1}, for which the gain on branches A and C is maximum, and assume that at $\tau=0$, $V_{01}=\psi/\gamma_0$ (on the helical trajectories $\psi=0$) and $V_{02}=(\xi^2-\psi^2)^{1/2}/\gamma_0$, so that as before $|\mathbf{V}_{01}||_{\tau=0}=\xi/\gamma_0$. The three curves in the figure correspond to $r\,|_{\tau=0}=0.868$ and $\psi=0,0.1,0.3$. Note that even for $\psi=0.3$ the reduction of the gain is not very significant, although the z dependence of the gain becomes more complex. Note also that in the examples in Fig. 3 the intensity of the radiation field is relatively weak and the nonlinear dependence of the gain is a result of the nonlinear dynamics of the beam in combined helical pump and axial guide magnetic fields. We demonstrate this nonlinear behavior in Fig. 4, where the time-averaged axial velocity V_{03} and radial displacement R of a typical electron trajectory are shown as functions of z in the cases $\psi=0$ (the dashed lines) and $\psi=0.3$ (solid lines). For $\psi=0.3$ we see the development of oscillations in V_{03} with the natural response frequency[7] and period of ~ 12 cm. The same frequency is present in the dependence on z of the radical displacement, where we also see additional rapid oscillations with the period of the helical field (~ 1 cm). Note that with an increase of ψ the radial displacements of the trajectories increase, which may lead to the violation of the conventional assumption in the theory that the beam is close to the axis of the magnetic wiggler. Increased radial excursions of the beam require inclusion of the radial component of the magnetic field of the wiggler and may result in additional destruction of the gain.

Finally, we discuss nonlinear saturation effects due to the radiation field itself. In the following example we assume that the beam initially is on branch A with $r=0.868$. The z dependence of the real parts of a_2 and a_3 for this case in the saturation phase, is shown in Fig. 5. The reason for the saturation in its initial stage becomes clear from Fig. 6, where the z dependence of V_{03}, V_{02}, and R is shown at saturation distances. We see in this figure that the saturation occurs mainly due to the destruction of the electron trajectory. The beam slows down, thus violating necessary conditions for the instability. In addition the radial excursions of the trajectories increase significantly.

It can be seen in Fig. 5 that at the late phase of the saturation, the amplitude of the electromagnetic field starts oscillating with increasing frequency as z increases. When the wavelength of these oscillations becomes comparable to the wavelength of the wave (~ 0.08 cm in the example in Fig. 5), inequality (12) is violated and our formulation becomes invalid for larger values of z. In Fig. 5 this happens at $z\sim 49$ cm. At this stage, new nonlinear effects occurring on a scale comparable with the wavelength of the electromagnetic wave may take place. One such effect is the trapping of the electrons in a strong ponderomotive potential. Our method cannot describe such effects and a more complicated approach, similar to that used in Refs. 11 and 12 must be applied at this stage. Nevertheless, the present theory is still valid at the onset of the saturation and describes its initial phase.

ACKNOWLEDGMENTS

This work was supported in part by the Office of Naval Research and by the National Science Foundation. The authors are also grateful to Mr. A. Fruchtman for his assistance in the numerical part of the work.

[1]T. C. Marshall, S.Talmage, and P. Efthimion, Appl. Phys. Lett. 31, 320 (1977).
[2]V. L. Granatstein, S. P. Schlesinger, M. Herndon, R. K. Parker, and J. A. Pasour, Appl. Phys. Lett. 30, 384 (1977).
[3]D. B. McDermott, T. C. Marshall, S. P. Schlesinger, R. K. Parker, and V. L. Granatstein, Phys. Rev. Lett. 41, 1368 (1978).
[4]R. M. Gilgenbach, T. C. Marshall, and S. P. Schlesinger, Phys. Fluids 22, 971 (1978).
[5]R. H. Jackson, R. K. Parker, and S. H. Gold, Bull. Am. Phys. Soc. 25, 947 (1980).
[6]S. H. Gold, P. H. Jackson, R. K. Parker, H. P. Freund, V. L. Granatstein, P. C. Efthimion, M. Herndon, and A. K. Kinkead, in *Physics of Quantum Electronics,* Vol. 9, edited by S. F. Jacobs, H. S. Piloff, M. Sargent, M. O. Scully, and R. Spitzer (Addison-Wesley, Reading, Mass., 1982), p. 741.
[7]L. Friedland, Phys. Fluids 23, 2376 (1980).
[8]L. Friedland and J. L. Hirshfield, Phys. Rev. Lett. 44, 1456 (1980).
[9]L. Friedland and I. B. Bernstein, Phys. Rev. A 23, 816 (1981).
[10]L. Friedland and A. Fruchtman, Phys. Rev. A 25, 2693 (1982).
[11]P. Sprangle, Cha-Mei Tang, and W. M. Manheimer, Phys. Rev. Lett. 43, 1932 (1979).
[12]P. Sprangle, Cha-Mei Tang, and W. M. Manheimer, Phys. Rev. A 21, 302 (1980).
[13]P. C. Liewer, A. T. Lin, and J. M. Dawson, Phys. Rev. A 23, 1251 (1981).